

See discussions, stats, and author profiles for this publication at: <https://www.researchgate.net/publication/264675120>

Carrier capture kinetics at electrical defects in poly [2-methoxy-5-(2'-ethyl-hexyloxy)-1,4-phenylenevinylene] (MEH-PPV) studied using charge transient spectroscopy

ARTICLE *in* JOURNAL OF APPLIED PHYSICS · AUGUST 2014

Impact Factor: 2.18 · DOI: 10.1063/1.4891832

CITATIONS

2

READS

29

3 AUTHORS:



Karanam Sudheendra Rao

Institute of Minerals and Materials Technology

9 PUBLICATIONS 5 CITATIONS

[SEE PROFILE](#)



Durgesh Chand Tripathi

Indian Institute of Technology Kanpur

15 PUBLICATIONS 32 CITATIONS

[SEE PROFILE](#)



Y. N. Mohapatra

Indian Institute of Technology Kanpur

111 PUBLICATIONS 643 CITATIONS

[SEE PROFILE](#)

Carrier capture kinetics at electrical defects in poly [2-methoxy-5-(2-ethyl-hexyloxy)-1,4-phenylenevinylene] (MEH-PPV) studied using charge transient spectroscopy

K. Sudheendra Rao, Durgesh C. Tripathi, and Y. N. Mohapatra

Citation: *Journal of Applied Physics* **116**, 054511 (2014); doi: 10.1063/1.4891832

View online: <http://dx.doi.org/10.1063/1.4891832>

View Table of Contents: <http://scitation.aip.org/content/aip/journal/jap/116/5?ver=pdfcov>

Published by the AIP Publishing

Articles you may be interested in

The red-phase of poly[2-methoxy-5-(2-ethylhexyloxy)-1,4-phenylenevinylene] (MEH-PPV): A disordered HJ-aggregate

J. Chem. Phys. **139**, 114903 (2013); 10.1063/1.4819906

Thickness dependent absorption and polaron photogeneration in poly-(2-methoxy-5-(2-ethyl-hexyloxy)-1,4-phenylene-vinylene)

J. Appl. Phys. **111**, 124512 (2012); 10.1063/1.4729770

Ionizing radiation induced degradation of poly (2-methoxy-5-(2'-ethyl-hexyloxy) -1,4-phenylene vinylene) in solution

J. Appl. Phys. **110**, 073510 (2011); 10.1063/1.3644946

Recombination profiles in poly[2-methoxy-5-(2-ethylhexyloxy)-1,4-phenylenevinylene] light-emitting electrochemical cells

J. Appl. Phys. **98**, 124907 (2005); 10.1063/1.2149162

Optoelectronic characteristics of polymer light emitting diodes with poly(2-methoxy-5-(2ethyl-hexyloxy)-1,4-phenylene-vinylene) and hydrogenated amorphous silicon alloy heterointerfaces

Appl. Phys. Lett. **81**, 205 (2002); 10.1063/1.1492310

**Advances in Live Single-Cell Thermal Imaging and Manipulation
International Symposium, November 10-12, 2014**

biophysics; soft condensed matter/soft mesoscopics; IR/terahertz spectroscopy
single-molecule optoelectronics/nanoplasmonics; photonics; living matter physics

Application deadline: August 24



OKINAWA INSTITUTE OF SCIENCE AND TECHNOLOGY GRADUATE UNIVERSITY
沖縄科学技術大学院大学

Carrier capture kinetics at electrical defects in poly [2-methoxy-5-(2'-ethyl-hexyloxy)-1,4-phenylenevinylene] (MEH-PPV) studied using charge transient spectroscopy

K. Sudheendra Rao,^{1,2} Durgesh C. Tripathi,^{1,2} and Y. N. Mohapatra^{1,2,3}

¹Department of Physics, Indian Institute of Technology Kanpur, Kanpur 208016, India

²Samtel Center for Display Technologies, Indian Institute of Technology Kanpur, Kanpur 208016, India

³Materials Science Programme, Indian Institute of Technology Kanpur, Kanpur 208016, India

(Received 2 June 2014; accepted 21 July 2014; published online 7 August 2014)

We use charge transient spectroscopy to study the trap levels in the prototypical polymeric semiconductor poly [2-methoxy-5-(2'-ethyl-hexyloxy)-1,4-phenylenevinylene] (MEH-PPV). Emission signature of the traps has been resolved using higher order spectroscopic analysis techniques of charge transients. The nature of the defect potential is best understood by studying capture mechanisms. Carrier capture kinetics of the dominant defects are studied using variable pulse-width filling technique to directly determine capture coefficients as a function of temperature. We demonstrate that charge redistribution occurs among the *discrete* traps through the process of multiple trapping and emission. Of the eight deep traps detected, the two dominant ones, christened T2 and T3, with activation energies of 0.38 and 0.49 eV are studied in detail. We go on to develop a phenomenological model representing the various activation energies in the mechanism of capture and emission. One of them involves a capture barrier of as high as 0.27 eV, indicating the occurrence of multi-phonon emission mechanism during capture. There is evidence to suggest that the dominant traps are different states of a defect from the same physical origin. © 2014 AIP Publishing LLC.

[<http://dx.doi.org/10.1063/1.4891832>]

I. INTRODUCTION

In organic semiconducting devices, the lifetime and degradation issues continue to remain as major concerns.^{1–11} The lifetime limiting processes for new generation of devices can often be linked to creation of defects and associated charge processes.^{9,12,13} However, unlike inorganic semiconductors, there are no clear methodologies for understanding of electrical defects in organic semiconductors. There have been earlier efforts to use the conventional techniques such as Thermally Stimulated Current (TSC),^{12–14} Deep Level Transient Spectroscopy (DLTS),^{15–22} and Deep Level Optical Spectroscopy (DLOS),^{23–27} to study these defects in organic semiconductors. However, the applicability and validity of standard methods are often questionable, since the physics of the charge processes at these defects are not well understood. For example, analysis valid for standard diodes cannot be used, since they are not based on variation of depletion width with bias. It is also not known to what extent the standard Shockley-Read-Hall (SRH) statistics is applicable for such materials and the significance of parameters involved. This has prevented monitoring the quality of material in terms of traps and their origin.^{2,3} There is currently a lack of clarity on whether the Density of States (DOS) of trap levels is discrete^{12–27} or continuous.^{3,28,29} Since the charge processes in organic semiconductors are slow processes, traditional measurement techniques seem to yield little results. In this paper, we demonstrate that by monitoring the charge transients over a large time scale and analyzing them using isothermal spectroscopic techniques, it is possible to estimate the occupancy of deep levels and various parameters associated with it, specifically the capture

cross-section. The kinetics of charge emission and capture are therefore studied spectroscopically by measuring the charge transients of a standard conjugated polymer, poly [2-methoxy-5-(2'-ethyl-hexyloxy)-1,4-phenylenevinylene] (MEH-PPV) diode varying the duration of charging time and pulse amplitude.

There have been early studies on MEH-PPV using transient and DLTS family of techniques employing Schottky structures and p-n junctions with n-Si as the substrate.^{15,16,30} Stallinga *et al.*¹⁶ used such structures to report the existence of two hole traps (with activation energies at 0.48 eV and 1.3 eV) and two electron traps (0.3 eV and 1.0 eV). Nguyen *et al.*^{31,32} have reported dominant deep levels between 0.3 eV and 0.4 eV of uncertain origin using charge DLTS. There have also been reports of non-exponential emission from traps in these organic semiconducting materials.^{13,33} However, no coherent view of nature of commonly occurring midgap states (beyond reporting activation energies of bunch of deep states) through spectroscopic resolution or their capture kinetics have been attempted as yet. It is important to pursue the physics underlying the trap kinetics in these polymeric materials, and MEH-PPV is an appropriate choice for mounting such a study. A long term objective would be to model the defect potential involved at such traps.³⁴ It is interesting to note that recently the involvement of a deep trap has been proposed in the formation of bi-polarons through optically detected magnetic resonance studies. An understanding of carrier capture kinetics can unravel possible role that such a defect plays in bi-polaron formation. Moreover, the knowledge of specific trap parameters such as energy, capture cross-section and concentration helps in estimating recombination process. Hence, an understanding of

charge process at these defects and their origin in material or process facilitates improving diode characteristics.

In this paper, we identify deep traps in MEH-PPV using higher order isothermal charge transient spectroscopy. We show that the most of the defects are discrete in energy and study the capture kinetics directly at the dominant ones. The activation energies involved in the process of capture and emission are derived. The origin and role of these dominant defects are discussed. In Sec. II, we provide the details of sample fabrication and spectroscopic techniques of analysis of transients. In Sec. III, we first focus on identification on the basis of emission signature and then follow up to monitor their occupancy to study capture kinetics, leading to a discussion on possible origin and physical signature of the results.

II. EXPERIMENTAL DETAILS

All the results in this study use a simple diode having the structure ITO|PEDOT:PSS|MEH-PPV|Al. For the current study, we used high purity MEH-PPV obtained from commercial sources. Properly cleaned indium tin oxide (ITO) coated substrates were patterned using the standard photo-lithography technique, followed by cleaning in RCA solution. Subsequently, pixelization was done to define the actual active area of the device. These pixelized ITO substrates were heated on a hot plate at 140 °C for 2 h in air. Thereafter, substrates were treated in UV-ozone for improving the ITO work function and removing undesirable residuals from the surface. A thin layer of polyethylene dioxythiophene: polystyrene sulfonate (PEDOT:PSS), purchased from the Bayer Corporation, was spin-coated to get a layer thickness ~75 nm and then dried at 120 °C for 1 h under a vacuum of ~10⁻⁶ mbar. The active layer of MEH-PPV (solution of 6 mg/cc) was spin-coated to obtain ~100 nm thickness by using the appropriate spin speed, and the substrates were transferred to the vacuum chamber for drying at 120 °C for around 90 min. Subsequently, aluminium (Al), as the cathode layer, was deposited at a rate of 1 Å/s through a shadow mask. A simple diode having the structure ITO|PEDOT:PSS|MEH-PPV|Al with circular active area of diameter 4 mm was used in this study. The fabrication of devices has been especially optimized for low leakage current, as charge transients were very sensitive to any leakage current.

The principle of transient experiments lies in creating a non-equilibrium occupancy of the traps and monitor their return to equilibrium under controlled conditions. In a typical charge transient experiment, the diode is charged for a specified duration by applying a forward bias and then the bias is removed to monitor the charge emission from the device as a function of time. A special purpose charge-to-voltage converter based on a charge integrator was developed in-house and interfaced to an oscilloscope (Agilent 54615B/MSO6012A) to measure the charge transients. The transients were acquired over several decades in time scale (from 5 μs to 20 s) by stitching together two transients from the oscilloscope with varying sampling times.

Time analyzed transient spectroscopy (TATS) technique is an isothermal variant of traditional DLTS. A first-order

TATS signal is constructed from the difference of the values of the transient at two different, correlated times. The first order TATS signal for a voltage transient $V(t)$ is given by

$$S_1(t) = V(t + \gamma t) - V(t), \quad (1)$$

where γ is an experimentally selectable constant. When first order TATS signal is plotted against the logarithm of the time, an exponential signal would go through a maximum or minimum, whose peak height is proportional to the amplitude, and the time of occurrence is proportional to the time constant of the exponential. However, during the course of this work, use of first-order TATS failed to resolve the closely lying peaks, some time leading to the conclusion that the energy levels may be distributed. Hence, we resort to second order TATS. The second-order TATS signal for a voltage transient $V(t)$ is given by

$$S_2(t) = V(t) - 1.5V((1 + \gamma)t) + 0.5V((1 + \gamma)^2t), \quad (2)$$

where γ is an experimentally chosen constant. Second order TATS signal of acquired charge transient is plotted, and subsequently, data are fitted with multiple identified exponentials characterized by their emission time constants. From the fittings, the amplitude of each exponent is identified, which is converted into charge based on the capacitor used for charge integration to obtain the occupied carrier concentration. It is important to reiterate that first order transient is a two point correlator or can be thought of as a moving window correlator. In contrast, second order TATS-S₂(t) is a three point correlator which has better resolving power at the cost of being more sensitive to noise in the signal.

III. RESULTS AND DISCUSSION

As explained earlier, the prepared devices need to meet the requirements by showing good rectification and then only can be used for the study of the trap states in these materials. Figure 1 shows a typical current density-voltage

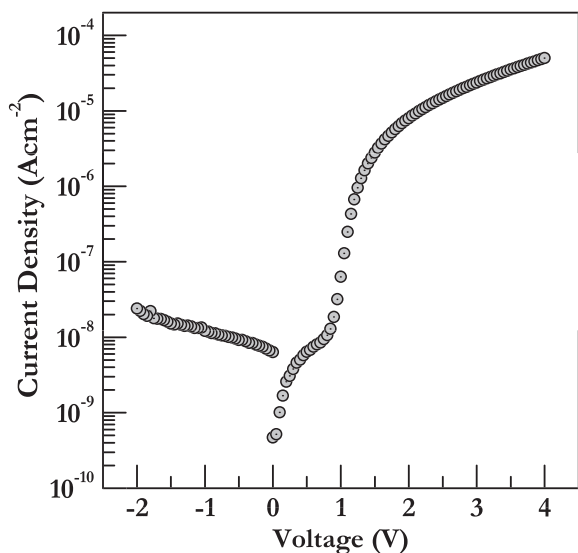


FIG. 1. Typical current-voltage characteristics of the studied device (with low leakage and good rectification) with the structure ITO|PEDOT:PSS|MEH-PPV|Al, which is used for all the measurements reported in this study.

(J-V) characteristic of a diode suitable as device under test with low reverse leakage, and a sharp exponential region before the space charge limited current sets in. As the measurements involve the integration of charge emitted from the trap levels, low leakage current is primary requirement. Therefore, a good rectification ratio is highly desirable in these studies.

A. Trap levels in MEH-PPV based diodes

1. Identification of trap level distribution

The measurement of time constant of emission as a function of temperature constitutes electrical signature of localized traps.³⁵ A judicious choice of filling time and injected concentration of carriers is required to get the best possible resolution of emission time constants. The magnitude of carrier concentration is conveniently controlled by forward bias, and the width of the filling pulse controls capture duration. Figure 2 shows three normalized curves for different combinations of the two parameters (i.e., forward bias and filling time). For low bias and small fill times, the signal-to-noise ratio of the TATS signal sets a lower limit of detection of approximately 10^{13} cm^{-3} , which can be made even lower by a suitable choice of components (specially the integrating capacitor) in the setup. With the help of small bias and large fill times, we are able to observe multiple distinguishable peaks as shown in Fig. 2 at a convenient temperature of 299 K. This is due to small amount of charge being injected into device for large times lead to steady state occupancy of all possible trap levels, which emit on removal of the forward bias. By following the variation of control parameters (bias, fill time, and temperature), we identify eight different peaks,³⁶ of which five peaks could clearly be resolved and studied in detail. The room temperature emission time constants of these levels named T1–T5 are listed in

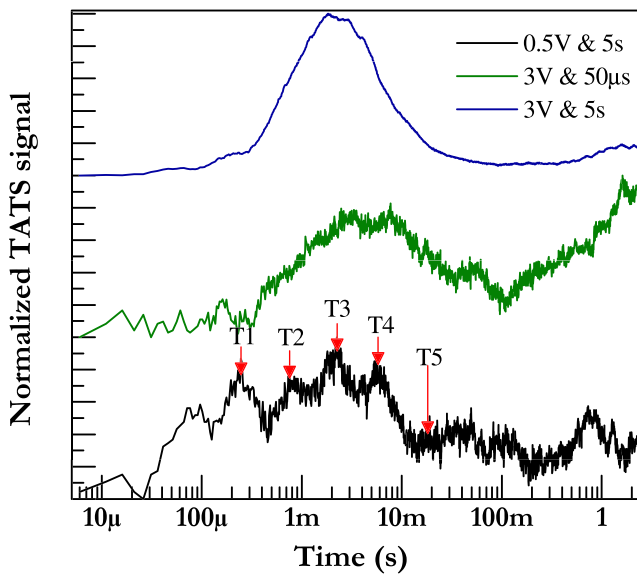


FIG. 2. Normalized TATS-S₂ signal of charge transients to identify the trap levels (all are isothermal transients which were acquired at 299 K). Five levels T1 to T5 have been marked. Some of the peaks (can be seen distinctively in the lowest curve) are not considered for analysis as their height did not change with bias or fill time.

TABLE I. Emission time constant and their activation energies of various identified trap levels.

Trap name	Emission time constant (at 299 K)	Activation energy (eV)
T1	228 μs	0.23
T2	880 μs	0.38
T3	2.1 ms	0.49
T4	5.5 ms	0.57
T5	20 ms	1.08

Table I for the convenience of identification by other workers. Using a series of isothermal transients, the occurrences of the identified peaks are tracked at several temperatures between 250 K and 315 K. Analysis using first order TATS, as has been previously reported in the literature,³² proved to be inadequate for resolving the trap levels.

2. Emission kinetics

Figure 3 shows TATS-S₂ signal of charge transients obtained for a 2.5 V bias and a 2 s filling pulse as a typical example of movement of peak positions with temperature. The peak height varies non-monotonically for the same trap - an important issue we take up in a later section. From detailed balance and phenomenological model of SRH statistics of traps, it is well known that the charge emission rate, for example, from a single hole trap level, e_p is given by

$$e_p = c_p N_M e^{-\left(\frac{E_A}{k_B T}\right)}, \quad (3)$$

where c_p is the capture coefficient, N_M is the total site concentration, E_A is the effective energy gap, and T is the temperature. We have not considered any explicit temperature dependence of the pre-exponential term. In inorganic semiconductor literature, often T^2 in the pre-exponential is considered arising out of product of effective density of states and thermal velocity. The activation trap energy of the identified

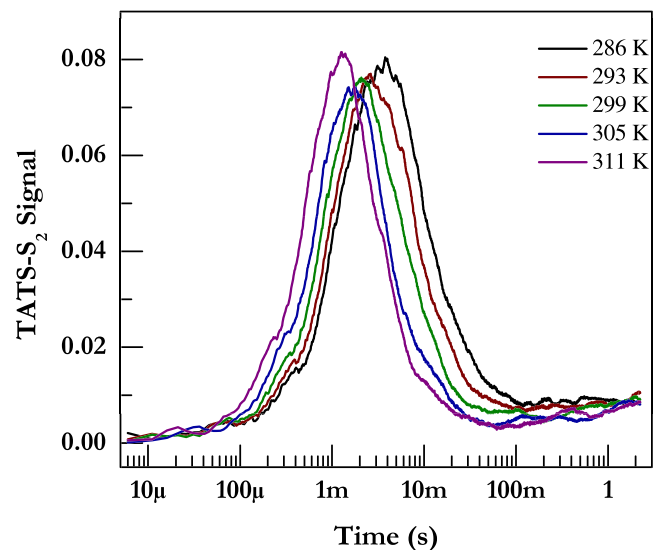


FIG. 3. TATS signal as a function of temperature for the fill times of 2 s and at 2.5 V bias.

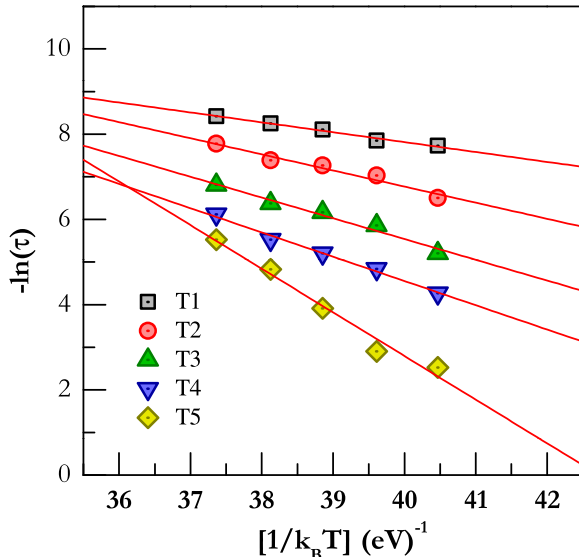


FIG. 4. Arrhenius plot of emission time to extract the activation energy of various identified trap levels. (Trap concentrations have been obtained from the fittings of Fig. 3.)

traps is obtained from the Arrhenius plot of the observed emission time constants from the peak positions. The typical Arrhenius plot for five of the traps of sufficient concentration within the temperature window are shown in Fig. 4, and the corresponding activation energies are listed in Table I.

In similar analysis for inorganic semiconductors, the pre-exponential in Eq. (3) is given as $\sigma_p \langle v_{th} \rangle N_v$, where σ_p is the capture cross-section, $\langle v_{th} \rangle$ is the average thermal velocity, and N_v is the effective density of states to which carriers are emitted. Hence, in traditional analysis, the y-intercept of the Arrhenius straight line can give a measure of cross-section knowing the average thermal velocity and the effective density of states, which in turn depends on the effective mass of the carrier. However, some of the ideas on the density of states of band and effective mass of the carrier and the average thermal velocity cannot be directly borrowed to the case of *organic semiconductors*, since they are amorphous and the carriers involved are not Bloch states as in the case of traditional band semiconductors. Further, such intercepts are extremely sensitive to slight changes in the slope and one can make errors of several orders estimating them from typical narrow temperature window in which measurements are carried out. Hence, we refrain from using the intercepts to conclude anything specific, though Nguyen *et al.*³² and other workers^{37,38} have used the Arrhenius plots to extract the capture cross section. However, the plots themselves are certainly usable as electrical signature of the specific defects. Instead we attempt to measure capture cross-section from direct measurements of occupancy with filling time in a later section. It is also important to measure the capture cross-section as a function of temperature since such dependences reveal the physics of mechanisms and the nature of the potentials involved at the trapping sites.

Using first order TATS, we had often observed non-exponential transients in similar samples. The significance of observation of a bunch of discrete states through higher order spectroscopy confirms that the prior observation of

non-exponential transients must be due to a summation of exponential transients from many emitting centers. It is known that such a sum from multiple states can indeed lead to stretched exponentials.

3. Trap occupancy: Bias dependence

Increase in forward bias during the filling primarily increases the carrier capture rate ($c_p p$ for a hole trap, where p is the free hole concentration), since larger concentration of carriers are injected. TATS signal of charge transients obtained for various biases, with the same fill time of 5 s and at temperature 299 K has been shown in Fig. 5. The spectrum gets dominated by the trap T3 which occurs in largest concentration though all other traps are clearly observed. The amplitude of the overall TATS-S₂ signal rises rapidly with bias and peaks at around 2 V and falls beyond 2 V even though the fall is marginal. The spectra are fitted using emission time constants already obtained to extract the concentration of the defects.

Figure 6 shows occupied trap concentration of various identified trap levels as a function of the magnitude of the filling pulse. The filling time is kept large at 5 s so that nearly equilibrium occupations are reached for each level of hole injection. We can observe that the T3 trap concentration peaks for 2 V bias. The dominant peaks are T2, T3, T4, and T5; the others have very small amplitude even at 3 V filling pulse. The observation of the non-monotonic change in concentration with increasing bias is intriguing at the first sight.

But as we will see in the Sec. III A 4, since the duration of filling is much larger than the time constants of emission, the equilibrium occupancy of the traps is achieved through a competition between capture and emission. As a result, there is a redistribution of charges among multiple defects leading to non-monotonic behavior. One of the dominant noteworthy features is that for higher levels of injection, the

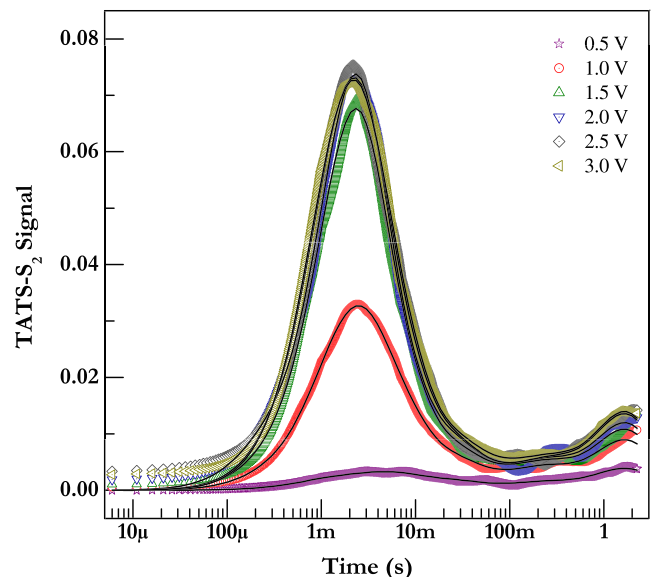


FIG. 5. TATS-S₂ signal as a function of bias for the fill times of 5 s and at a temperature 299 K. Symbols show the actual acquired data and the line through the data shows the fitting.

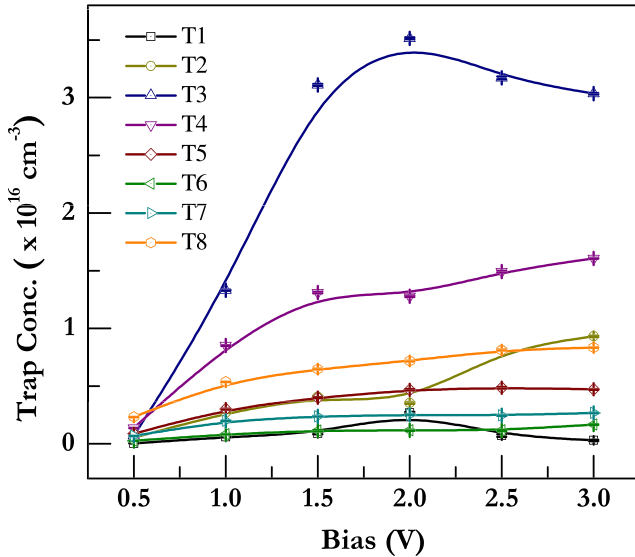


FIG. 6. Occupied trap concentration (extracted from TATS signal shown in Fig. 5) as a function of bias. Symbols show the actual acquired data and the line through the data is just a guide to eye. (Note that this graph has all the eight levels.)

trap T3 appears to be losing charges to a shallower trap T2 and deeper trap T4. This hints towards a possible common origin to the trap level T2, T3, and T4. For example, T3 could be a metastable state converting to either T2 or T4 as capture proceeds. Nonetheless, these results are a strong indication that the dominant traps share the same physical origin, possibly being the different states of the same defect, an issue we discuss in a later section.

4. Capture coefficient and charge redistribution

Capture kinetics are analyzed using TATS-S₂ signal of the charge transients at a given bias and a particular temperature by varying the fill-pulse width over six orders of magnitude from 50 μs to 5 s. The observed concentrations of emitting centers are obtained from the respective peak heights of the spectrum. Figure 7 shows TATS-S₂ signal and its fittings for different fill times at a temperature of 299 K, and a filling bias of 3 V. For purposes of clarity in the graph, some of the intermediate values of fill times have been not been shown in this figure.

Occupied trap concentration as a function of logarithmic fill time is shown in Fig. 8. It is clear from the figure that occupancy of most of the dominant trap levels is non-monotonic. Initially, the occupancy rises rapidly as the process is dominated by capture. But as the fill time increases more than the emission time constants, the loss of charges due to emission during fill time is no longer negligible. For example, the time dependence of single level occupancy of a trap would be determined by the rate equation

$$\frac{dp_T}{dt} = c_p p(N_T - p_T) - e_p p_T = c_p p N_T - (c_p p + e_p) p_T, \quad (4)$$

where N_T is the maximum trap concentration and p_T is the occupied trap concentration. For multiple traps, this would lead to set of coupled equations.

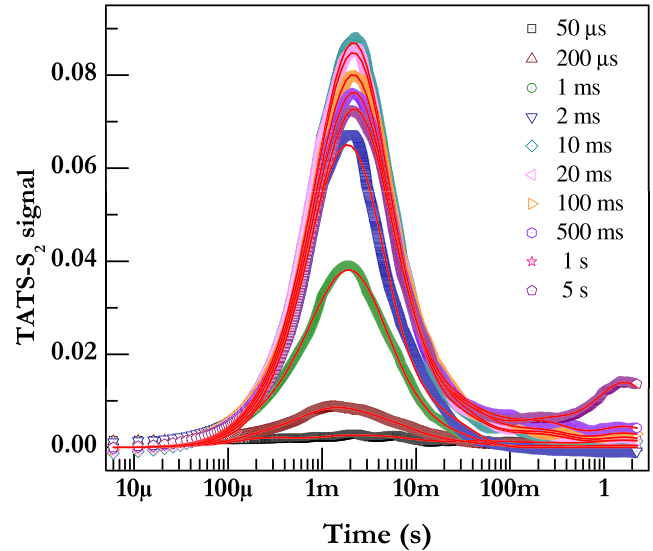


FIG. 7. TATS-S₂ signal and its fitting as a function of fill times at 3 V bias and at temperature 299 K.

Hence, the occupancy of any particular trap will increase at a combined rate of emission and capture rate reaching a steady state determined by both the rates eventually. In the presence of multiple traps, the shallower defects will lose the charge to deeper defects since the latter will have much smaller emission time constants. With increasing filling time beyond the emission time constants, we can observe decrease in occupancy of a shallower trap and corresponding increase in deeper traps due to multiple trapping and emission proceeding simultaneously as schematically shown in Fig. 9. In effect, the competition between capture and emission appears as progressive deepening of occupancy. This phenomenon of deepening of the charge distribution, termed as charge redistribution, has been observed in many systems and is well documented for defect dominated materials in inorganic semiconductors.³⁹ The signature of multiple trapping charge distribution is the occurrence of a

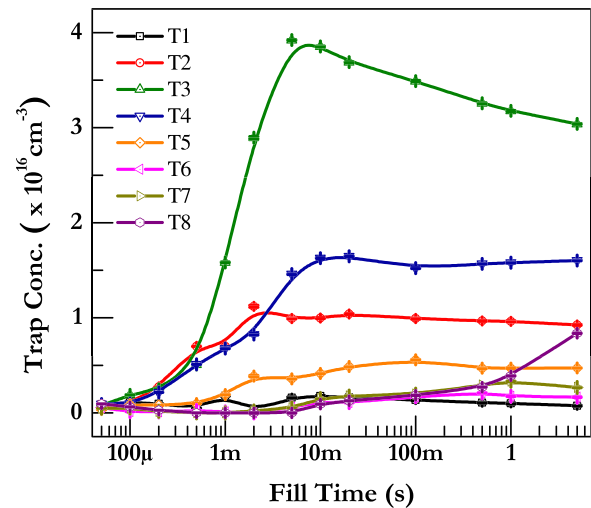


FIG. 8. Occupied trap concentration (extracted from TATS-S₂ signal shown in Fig. 7) as a function of fill times at 3 V bias and at temperature 299 K. Symbols show the actual acquired data and the line through the data is a guide to the eye.

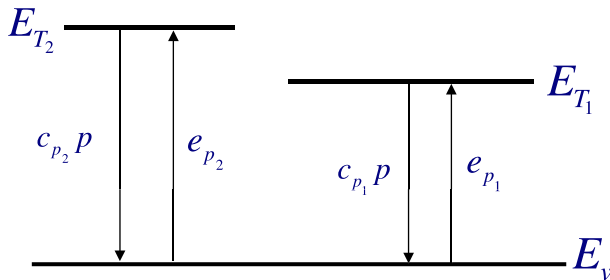


FIG. 9. Schematic of charge redistribution through multiple trapping of two hole levels through hole emission to and capture from the HOMO level represented as E_v . The direction of transitions is shown as per convention in Shockley-Read-Hall kinetics in inorganic semiconductors.

TABLE II. Capture time constant and trap densities of various identified trap levels. T1 concentration was too small to be able to estimate capture time constant.

Trap name	Capture time constant (at 3 V bias) (ms)	Trap concentration (N_T) ($\times 10^{15} \text{ cm}^{-3}$)
T2	1.0	17
T3	3.4	39
T4	5.5	16
T5	13.4	5.8

peak in concentration of a shallower trap approximately at a time of its emission time constant as is observed in Fig. 8.

The capture time constants can be calculated from these data assuming exponential increase in occupation at small times. Identified trap concentrations and capture time constants (at 3 V bias) of the dominant traps are listed in Table II, which were not possible for all the trap levels (especially levels at which significant redistribution is taking place). The maximum trap concentration (N_T) and the capture time constant can be easily identified by inspecting the peak values at all possible biases and temperatures. However, one needs an explicit knowledge of the carrier concentration during capture in each case to extract the capture cross section which is the physically meaningful quantity characterizing the trap.

5. Measuring capture cross-section

The knowledge of the capture cross-section is of importance, since it leads to mechanisms and physics behind carrier kinetics. As indicated earlier, inferring it from Arrhenius plot is unreliable both because of difficulty in estimating the intercept from interpolation, and due to conceptual problems associated with its interpretation in the case of amorphous organic semiconductors. Though we could monitor the capture process directly through evolution of occupancy, the capture cross section could not be directly estimated because of the complexity of redistribution of charges among the discrete states.

We propose an alternative method to estimate the capture cross section. In case of inorganic semiconductors, the capture coefficient is given by

$$c_p = \sigma_p \langle v_T \rangle, \quad (5)$$

where σ_p is the capture cross section and $\langle v_T \rangle$ is the average thermal velocity. This has been extended to calculate the

capture cross section even for organic materials by different groups.^{32,40,41} It has recently been shown by Kuik *et al.*⁴² and Sinha and Mohapatra⁴³ that the actual capture process is mobility dependent in the case of low-mobility organic materials. Hence, we propose that capture coefficient is limited by the drift velocity and use it instead of thermal velocity which can be written as

$$c_p = \sigma_p \langle v_d \rangle = \sigma_p \mu_p F, \quad (6)$$

where $\langle v_d \rangle$ is the average drift velocity, μ_p is the hole mobility, and F is the electric field. Neglecting diffusion contribution, we can assume that the measured current density for a given bias will be

$$J = qp\mu_p F, \quad (7)$$

where q is the fundamental charge, p is the hole density, μ_p is the hole mobility, and F is the average electric field neglecting its variation for simplicity. Using Eqs. (6) and (7), we can calculate the reciprocal of capture time constant which is given by

$$\frac{1}{\tau_c} = c_p p = \frac{\sigma_p J}{q}. \quad (8)$$

Thus, by measuring the capture time constant at each bias and by plotting it against the current density would give us the capture cross section. Figure 10 shows reciprocal of the capture time constant versus current density plot for the dominant traps T2, T3, T4, and T5. From the plot, the extracted capture cross sections at 299 K are listed in Table III. These values are much larger when compared to values reported by Nguyen *et al.*³² This is expected because the values they have extracted are from the conventional inorganic semiconductor model, where as we have used drift limited capture model. Do note that since the mobility is temperature dependent for most organic semiconductors, capture coefficient will also be temperature dependent. The method

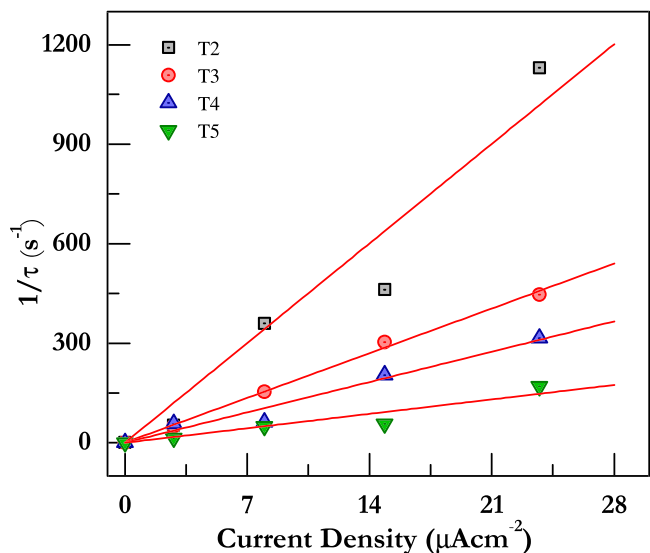


FIG. 10. Reciprocal of capture time constant versus the current density of the trap levels T2, T3, T4, and T5. Solid lines are linear fit to the data.

TABLE III. Capture cross section of the dominant peaks at 299 K.

Trap name	Capture cross section at 299 K ($\times 10^{-12} \text{ cm}^2$)
T2	6.9
T3	3.1
T4	2.1
T5	1.0

proposed here obviates the need for explicit knowledge of carrier concentration or mobility, and the straight line fits we get in Fig. 10 validate our basic approach.

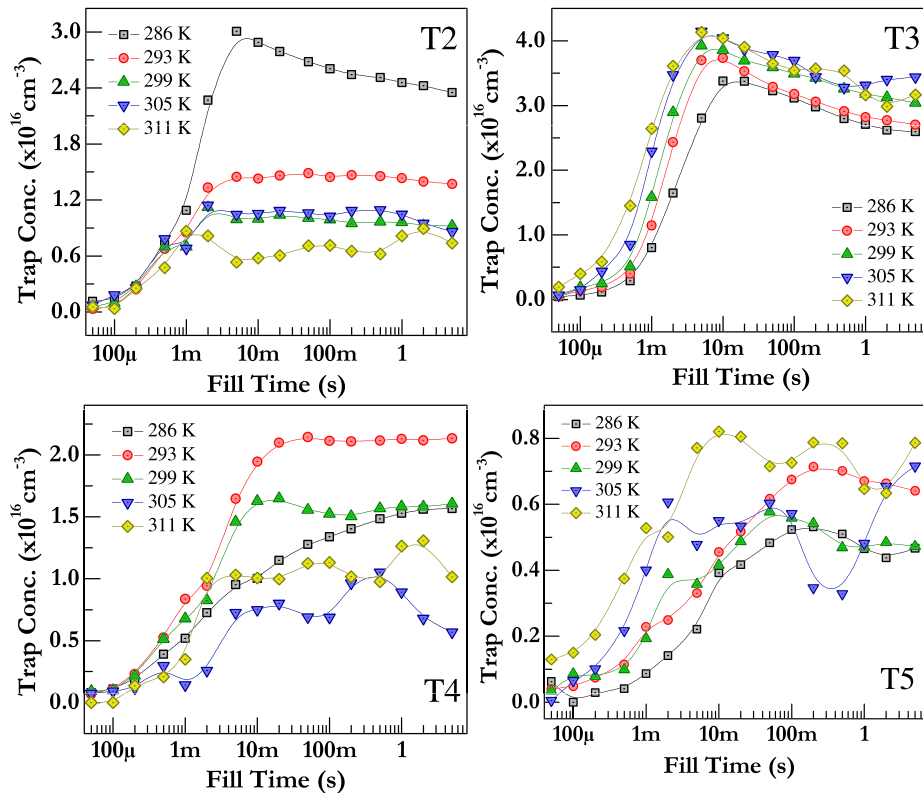
6. Temperature dependence of capture cross-section

Figure 11 shows the occupation concentration of the trap states as a function of fill time at different temperatures. For the case of trap level T2, we can see that the capture process is independent of temperature, even though the maximum filled states for lower temperatures increases. This is understandable as the thermal emission from the trap level is lowered at low temperatures. But the charges are also emitted beyond the emission time constant which can be specially noted at 287 K.

In case of trap level T3, we can see that the capture process is thermally activated as the occupation curves are shifted to lower times for lower temperatures. For thermally activated capture process, we would expect the cross section to be of the form

$$\sigma_p = \sigma_{p_\infty} e^{-(E_B/k_B T)}, \quad (9)$$

where E_B is capture barrier and σ_{p_∞} is the capture cross section at the high temperature limit. The variation is systematic



and redistribution of the carriers is observed consistently for each temperature beyond the emission time constant. However, for early times before the peak, the process is capture dominated. Hence, by plotting natural logarithm of $(N_T - p_T)$ vs fill time and calculating the slope would give us the capture constant as shown in Fig. 12(a). Invoking Eq. (8) and knowing current density gives us directly capture cross-section. Figure 12(b) shows the Arrhenius plot of the capture cross section, whose slope yields the capture barrier. In this case, the barrier E_B is found to be 0.27 eV.

In the case of T4 and T5, we can observe that the capture process is temperature dependent. But concentrations fluctuate due to redistribution, and it is not possible to estimate the capture cross section and the capture barrier by the method proposed. In any case, the temperature and filling time dependence of each of these dominant levels are laid bare in these set of curves.

B. Phenomenological model

For equilibrium carriers, the existence of mobility-gap between localized states and transport states is well-known from Bässler's formalism.^{44–46} In this formalism, for a Gaussian DOS of the LUMO with variance of σ , the equilibrium energy (E_{eq}) at a temperature T is given by $-\sigma^2/k_B T$ with the maximum of the Gaussian as the reference level. The transport energy level (E_{Tr}) beyond which carriers participate in conduction is given by $-5\sigma^2/9k_B T$. The gap between the two is called mobility gap (ΔE_μ) which is $4\sigma^2/9k_B T$ which makes the mobility temperature dependent with a variable energy gap. The energy level scheme within the DOS is shown in Fig. 13. If we assume the variance (σ) to be of the order of 100 meV, then the mobility gap will be

FIG. 11. Occupied trap concentration of dominant traps (extracted from TATS-S₂ signal shown in Fig. 7) as a function of fill times at 3 V bias for different temperatures. Symbols show the actual acquired data and the line through the data is just a guide to eye.

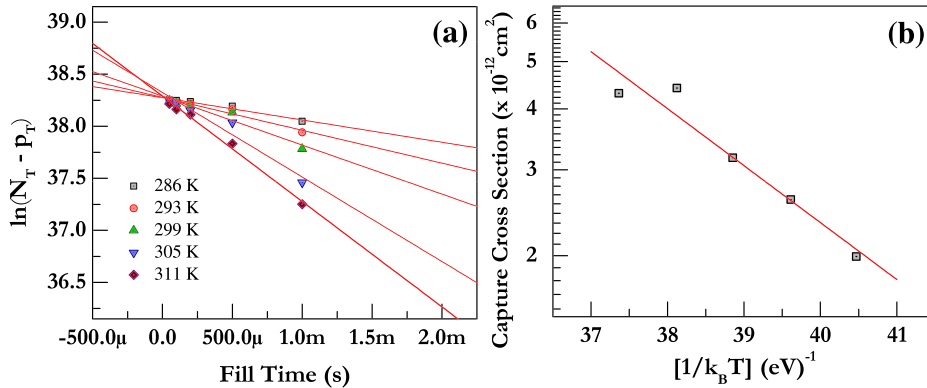


FIG. 12. (a) Natural logarithm of difference of total trap concentration and occupied trap concentration as a function of fill times at 3 V bias for different temperatures for the trap level T3. (b) Arrhenius plot of capture cross section. In both the cases, symbols represent experimental data and the lines are straight line fits.

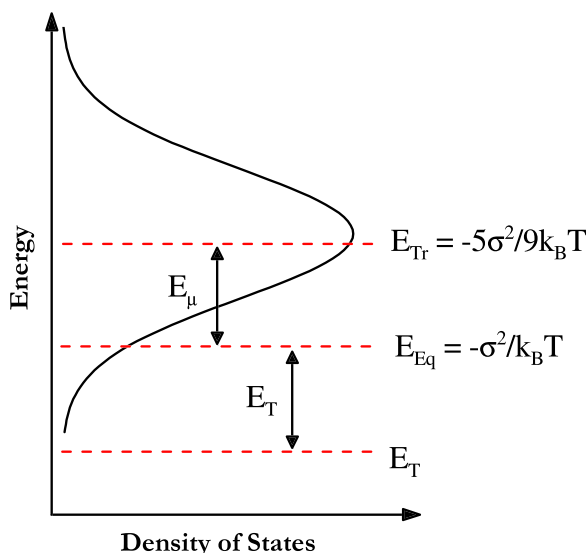


FIG. 13. Transport level (E_{Tr}), Equilibrium energy (E_{eq}) and trap energy (E_T) shown for a typical LUMO with the reference being at the maximum of distribution.

TABLE IV. Activation energy (E_A), capture barrier (E_B), and the actual trap energy (E_T).

Trap number	E_A (meV)	E_B (meV)	E_T (meV)
T2	380	0	210
T3	490	270	50

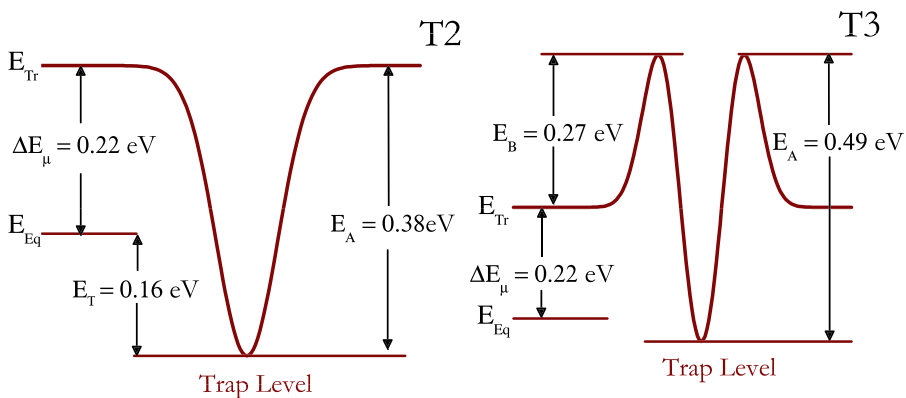


FIG. 14. Graphical representation energies measured E_A , E_B , and E_T along with ΔE_μ to understand the trapping phenomenon.

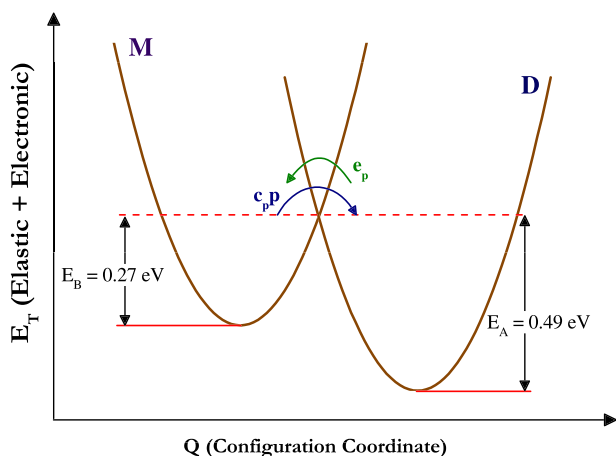


FIG. 15. A schematic configuration co-ordinate diagram showing emission activation energy and capture barrier. M is the state of the molecule with carrier in the transport state, and D is the T3 trapped state.

of multiple local phonons (violent vibrations) before it can get captured. The mechanism is known as multi-phonon emission model of capture. This is expected when the defect center goes through a structural distortion or change in mean position of the configuration co-ordinate through the process of carrier capture. The nature of the potential for T2 seems to be attractive and long range, while that of T3 as repulsive and short-range. All the other traps whose capture cross-section is clearly temperature dependent seem to share the character of T3.

C. Origin and significance of discrete states

Our effort in this work has been more to put electrical identification and determination of associated trap parameters (N_T , E_A , and σ_p , etc.) of deep defects in organic semiconductors on a firm physical basis using transient techniques. This is supposed to be of considerable help in the larger motivation of relating the electrical signature of the defects to their origin through process induced mechanisms, degradation, or even deliberate doping or introduction of embedded quantum structures. The latter motivation is often impeded by lack of reliable electrical studies so far.

For the case of MEH-PPV, we can relate some of our results to those already reported in the literature. It must be borne in mind though that the material quality and the control on device fabrication have improved considerably over the decade. Our experience also shows that unless due care is taken, even the samples fabricated in the same laboratory give different sets of defects. However, we have chosen commercial MEH-PPV in this study primarily because the material quality has now stabilized and it is possible to hone one's techniques and derive intrinsic physics from the results on this prototypical material.

Most studies using charge-DLTS, transient capacitance technique or thermally stimulated capacitance have only been successful in reporting a bunch of activation energies as deep level defects. Proceeding beyond determination of activation energy has been primarily problematic because of the absence of enough resolving power and sensitivity in detecting them electrically. After a perusal of the previous

studies, it appears that a hole trap between 0.4 and 0.5 eV^{13,15,16,31} as a dominant deep defect is a common observation. We attribute it to traps T2 and T3 clearly resolved using TATS-S₂ in our case. We believe that these two dominant states are intrinsic to MEH-PPV and are observed to occur in concentrations of 10^{16} cm^{-3} .

There has been a proposal that the formation of bipolarons, observed in MEH-PPV using electrically detected magnetic resonance, is mediated by traps with activation energy at 0.4 eV above the HOMO level.³⁴ The capture of the first hole (polaron) corresponds to T2 with activation energy of 0.38 eV. The observation of capture barrier E_B (0.27 eV) points to T3 being a repulsive site for capture of the second hole (polaron). The strong electron-phonon coupling in these systems though ensures that the capture of a second polaron will lead to overall energy minimization to 0.49 eV, which is the activation energy of trap T3. The site correlation energy will then be about 0.11 eV. The defect centre may then be considered as a negative U centre,^{39,47–49} in which the Coulombic repulsion energy at the site is overcome by overall distortion of the defect molecule in attaining a lower energy stable state. The two dominant states T2 and T3 can be considered to be arising from the same defect with two charge states. In fact, as speculated in Sec. III A 3, T3 may also be a metastable state of the same defect converting to either shallower trap T2 on emitting a hole, or a fraction getting stabilized as T4.

More generally, multiple discrete midgap states in large concentrations seem to be an intrinsic feature of MEH-PPV thin films. Most of the eight traps observed here are believed to be hole traps, since our devices inject copious holes from the ITO side. The injected electrons from the cathode are limited to few layers near the metal. The observed states are unlikely to be from interfaces since one expects interface states to be continuously distributed. The deepest level at about 1.0 eV may be an electron trap originating from the cathode side. However, more critical studies are required by making electron only devices to confirm any such identification.

The observation of large capture cross-section of the order 10^{-12} cm^2 also points to the fact that most deep defects in the material are Coulombic in origin. However, the actual carrier capture kinetics are slow in spite of having long range influence since the velocity with which carriers approach these centers are limited by the carrier drift velocity in these low-mobility materials as compared to that of thermal velocity in traditional crystalline semiconductors.

There seems to be near unanimity in the limited number of studies so far including ours that the deep level defects in MEH-PPV are discrete in nature and any observation of non-exponentiality or non-Debye relaxation reflects one's inability to resolve multiple emitting centers. A significant question is then the origin of the discrete nature of states in the HOMO-LUMO gap in spite of the disorder and randomness in the environment of each defect, especially if the range of the defect potential is large being Columbic in nature. It must be borne in mind though that the solid is an aggregation of molecules with weak van der Waals interaction. In a typical conjugated polymer, the electronic properties

saturate beyond a conjugation length of about dozen monomers. The π - π interaction among neighboring molecules gives rise to broadening of HOMO or LUMO levels, the tail of which below equilibrium energies can be considered as localizing traps. But, they are certainly not the deep level defects that we observe in charge transient experiments. It is unlikely therefore that mere change in conjugation length can produce deep and discrete levels. The origin of discrete midgap states should therefore be due to very specific structural (such as aggregates) or chemical species (such as undesirable groups attached to molecules). There have been several studies on oligomers containing specific number of monomers using optical spectroscopy in solution.^{50–52} Similar studies are not available for electrical studies in solids. The absence of energetic broadening suggests that the potential of such traps is deep tightly confining the carriers. This can, for example, occur for a monomer, or a dimer with two defects on either side in a chain. The electrical studies through capture cross-section can indeed reveal the nature of the potential well as has been shown here, and answer questions on the origin of such tightly binding traps.

IV. CONCLUDING REMARKS

To summarize, we have demonstrated the power of the second order TATS spectroscopy of charge transients in resolving discrete states, which seem to be a common feature in MEH-PPV. Of the eight deep traps detected, the two dominant ones, christened T2 and T3, with activation energies 0.38 and 0.49 eV could be resolved clearly. The kinetics of carrier capture at four of the traps are monitored at different temperatures and their capture cross-sections are estimated by assuming that capture is drift velocity limited in these materials. We also demonstrate that charge redistribution occurs among the discrete traps through the process of multiple trapping and emission. From the temperature dependence of capture constants we show that carrier capture at the dominant deep levels occur by overcoming energetic barriers. Phenomenological models to represent the measured activation energies are proposed for two of the dominant deep levels. One of them involves a capture barrier of as high as 0.27 eV indicating occurrence of multi-phonon emission mechanism during capture. We show evidence of the dominant traps being the states of defects with common physical origin.

A knowledge of trap parameters such as energy, concentration distribution (in terms of discrete or continuous and also actual numbers), capture coefficient, and possible interrelation among them at various conditions such as electrical stressing and environmental conditions would help in the identification of loss mechanisms. The ambitious objective of this line of investigation is, of course, is to be able to relate the nature of the localizing potential to their structural, or physico-chemical origin. The reliable and spectroscopic techniques based on second order TATS would certainly play a more fruitful role in the long term objective of relating defects, disorder, and degradation to the material quality, the fabrication processes and the performance limitations. Such

identification would eventually help in avoidance of undesirable traps and in the improvement of device applications.

ACKNOWLEDGMENTS

We are thankful to Department of Science and Technology, New Delhi for the financial support (DST/R&D/20060243).

- ¹Z. D. Popovic and H. Aziz, *IEEE J. Sel. Top. Quantum Electron.* **8**, 362 (2002).
- ²S. C. Xia, R. C. Kwong, V. I. Adamovich, M. S. Weaver, and J. J. Brown, in *Annual International Symposium on Reliability Physics* (2007), pp. 253–257.
- ³M. Roberts, K. Asada, M. Cass, C. Coward, S. King, A. Lee, M. Pintani, M. Ramon, and C. Foden, *Proc. SPIE* **7722**, 77220C (2010).
- ⁴R. A. Street, P. P. Khlyabich, and B. C. Thompson, *Org. Electron.* **14**, 2932 (2013).
- ⁵S. Schmidbauer, A. Hohenleutner, and B. Konig, *Adv. Mater.* **25**, 2114 (2013).
- ⁶R. Huber, F. Witt, H. Borchert, E. von Hauff, S. Heun, H. Buchholz, and J. Parisi, *J. Appl. Phys.* **113**, 023104 (2013).
- ⁷P. Kumar and S. Chand, *Prog. Photovoltaics: Res. Appl.* **20**, 377 (2012).
- ⁸N. Grossiord, J. M. Kroon, R. Andriessen, and P. W. M. Blom, *Org. Electron.* **13**, 432 (2012).
- ⁹I. R. de Moraes, S. Scholz, B. Lüssem, and K. Leo, *Org. Electron.* **12**, 341 (2011).
- ¹⁰F. So and D. Kondakov, *Adv. Mater.* **22**, 3762 (2010).
- ¹¹A. Pinato, A. Cester, M. Meneghini, N. Wrachien, A. Tazzoli, S. Xia, V. Adamovich, M. S. Weaver, J. J. Brown, E. Zanoni, and G. Meneghesso, *IEEE Trans. Electron Devices* **57**, 178 (2010).
- ¹²J. Steiger, S. Karg, R. Schmeichel, and H. von Seggern, *Synth. Met.* **122**, 49 (2001).
- ¹³V. Kazukauskas, *Semicond. Sci. Technol.* **19**, 1373 (2004).
- ¹⁴M. Meier, S. Karg, K. Zuleeg, W. Brutting, and M. Schwoerer, *J. Appl. Phys.* **84**, 87 (1998).
- ¹⁵H. L. Gomes, P. Stallinga, H. Rost, A. B. Holmes, M. G. Harrison, and R. H. Friend, *Appl. Phys. Lett.* **74**, 1144 (1999).
- ¹⁶P. Stallinga, H. L. Gomes, H. Rost, A. B. Holmes, M. G. Harrison, and R. H. Friend, *Synth. Met.* **111**, 535 (2000).
- ¹⁷O. Gaudin, R. B. Jackman, T.-P. Nguyen, and P. Le Rendu, *J. Appl. Phys.* **90**, 4196 (2001).
- ¹⁸S.-F. Chen and C.-W. Wang, *Appl. Phys. Lett.* **85**, 765 (2004).
- ¹⁹C.-H. Huang, C.-W. Lee, C.-S. Hsu, C. Renaud, and T.-P. Nguyen, *Thin Solid Films* **515**, 7671 (2007).
- ²⁰T. P. Nguyen, C. Renaud, P. L. Rendu, and S. H. Yang, *Phys. Status Solidi C* **6**, 1856 (2009).
- ²¹C. W. Lee, C. Renaud, P. Le Rendu, T. P. Nguyen, B. Seneclauze, R. Ziessl, H. Kanaan, and P. Jolinat, *Solid State Sci.* **12**, 1873 (2010).
- ²²C. Renaud, Y. Josse, C.-W. Lee, and T.-P. Nguyen, *J. Mater. Sci.: Mater. Electron.* **19**, S87 (2008).
- ²³Y. Nakano, K. Noda, H. Fujikawa, T. Morikawa, T. Ohwaki, and Y. Taga, *Appl. Phys. Lett.* **88**, 252104 (2006).
- ²⁴Y. Nakano, K. Noda, H. Fujikawa, and T. Morikawa, *Phys. Status Solidi (RRL)* **1**, 196 (2007).
- ²⁵Y. Nakano, K. Noda, H. Fujikawa, T. Morikawa, and T. Ohwaki, *J. Appl. Phys.* **46**, 2636 (2007).
- ²⁶Y. Nakano, K. Noda, H. Fujikawa, and T. Morikawa, *J. Appl. Phys.* **47**, 464 (2008).
- ²⁷Y. Nakano, *Appl. Phys. Express* **2**, 092103 (2009).
- ²⁸C. Féry, B. Racine, D. Vaufrey, H. Doyeux, and S. Cinà, *Appl. Phys. Lett.* **87**, 213502 (2005).
- ²⁹I. Thurzo, H. Méndez, and D. R. T. Zahn, *Phys. Status Solidi A* **202**, 1994 (2005).
- ³⁰P. Stallinga, H. L. Gomes, H. Rost, A. B. Holmes, M. G. Harrison, and R. H. Friend, *J. Appl. Phys.* **89**, 1713 (2001).
- ³¹T. P. Nguyen, *Mater. Sci. Semicond. Process.* **9**, 198 (2006).
- ³²T. P. Nguyen, P. Le Rendu, O. Gaudin, A. J. T. Lee, R. B. Jackman, and C. H. Huang, *Thin Solid Films* **511**, 338–341 (2006).
- ³³Y. S. Yang, S. H. Kim, J.-I. Lee, H. Y. Chu, L.-M. Do, H. Lee, J. Oh, T. Zyung, M. K. Ryu, and M. S. Jang, *Appl. Phys. Lett.* **80**, 1595 (2002).

- ³⁴J. Behrends, A. Schnegg, K. Lips, E. A. Thomsen, A. K. Pandey, I. D. W. Samuel, and D. J. Keeble, *Phys. Rev. Lett.* **105**, 176601 (2010).
- ³⁵S. Agarwal, Y. N. Mohapatra, and V. A. Singh, *J. Appl. Phys.* **77**, 3155 (1995).
- ³⁶The other three traps T6, T7, and T8 which occurred in very low concentrations were deeper traps with room temperature time constants as 55 ms, 205 ms, and 1.7 s, respectively.
- ³⁷D. Bozyigit, M. Jakob, O. Yarema, and V. Wood, *ACS Appl. Mater. Interfaces* **5**, 2915 (2013).
- ³⁸D. Bozyigit, S. Volk, O. Yarema, and V. Wood, *Nano Lett.* **13**, 5284 (2013).
- ³⁹P. Giri and Y. Mohapatra, *Phys. Rev. B* **62**, 2496 (2000).
- ⁴⁰J. Schafferhans, Ph.D. thesis, Universität Würzburg, 2011.
- ⁴¹T. P. Nguyen, C. Renaud, C. H. Huang, C.-N. Lo, C.-W. Lee, and C.-S. Hsu, *J. Mater. Sci.: Mater. Electron.* **19**, S92 (2008).
- ⁴²M. Kuik, L. J. Koster, G. A. Wetelaer, and P. W. Blom, *Phys. Rev. Lett.* **107**, 256805 (2011).
- ⁴³D. K. Sinha and Y. N. Mohapatra, *Org. Electron.* **13**, 1456 (2012).
- ⁴⁴V. I. Arkhipov, E. V. Emelianova, and H. Bässler, *Philos. Mag. B* **81**, 985 (2001).
- ⁴⁵V. I. Arkhipov, U. Wolf, and H. Bässler, *Phys. Rev. B* **59**, 7514 (1999).
- ⁴⁶H. Bässler, *Phys. Status Solidi B* **175**, 15 (1993).
- ⁴⁷G. D. Watkins and J. R. Troxell, *Phys. Rev. Lett.* **44**, 593 (1980).
- ⁴⁸S. T. Pantelides, *Deep Centers in Semiconductors* (Taylor & Francis, 1992).
- ⁴⁹P. W. Anderson, *Phys. Rev. Lett.* **34**, 953 (1975).
- ⁵⁰M. M. L. Grage, P. W. Wood, A. Ruseckas, T. Pullerits, W. Mitchell, P. L. Burn, I. D. W. Samuel, and V. Sundstrom, *J. Chem. Phys.* **118**, 7644 (2003).
- ⁵¹R. Chang, J. H. Hsu, W. S. Fann, K. K. Liang, C. H. Chang, M. Hayashi, J. Yu, S. H. Lin, E. C. Chang, K. R. Chuang, and S. A. Chen, *Chem. Phys. Lett.* **317**, 142 (2000).
- ⁵²M. S. Khoshkho, F. A. Taromi, E. Kowsari, and E. K. Shalamzari, *Polymer* **54**, 4017 (2013).